Journal of Organometallic Chemistry, 411 (1991) 419–430
Elsevier Sequoia S.A., Lausanne
JOM 21718

Some studies on dicyclohexylammonium hydridoundecacarbonyltriferrate *

R.B. King, G.S. Chorghade, N.K. Bhattacharyya
Department of Chemistry, University of Georgia, Athens, GA 30602 (USA)

E.M. Holt
Department of Chemistry, Oklahama State University, Stillwater, OK 74078 (USA)

and Gary J. Long
Department of Chemistry, University of Missouri-Rolla, Rolla, MO 65401 (USA)

(Received November 23rd, 1990)

Abstract

The salt $[Cx_2NH_2][HFe_3(CO)_{11}]\cdot OEt_2$ (Cx = cyclohexyl, Et = ethyl) was isolated from $Cx_2NBBr_2/Na_2Fe_2(CO)_8/Et_2O$ and was shown by X-ray diffraction (monoclinic, $P2_1/a$: $a = 17.449(5)$, $b = 16.345(5)$, $c = 13.466(4)$ Å, $\beta = 118.45(2)°$, $Z = 4$) to contain the expected $Cx_2NH_2^+$ and $HFe_3(CO)_{11}^-$ ions as well as the diethyl ether. In each $Cx_2NH_2^+$ cation one hydrogen atom is hydrogen bonded to the bridging CO oxygen of the $HFe_3(CO)_{11}^-$ anion whereas the other hydrogen atom is hydrogen bonded to the diethyl ether. The Mössbauer effect spectral parameters (δ, ΔE_Q, Γ, area ratios) of $[Cx_2NH_2][HFe_3(CO)_{11}]$ at 295 and 78 K are closely related to those of $Fe_3(CO)_{12}$.

Introduction

The $HFe_3(CO)_{11}^-$ anion (I) is a relatively stable and readily available metal carbonyl anion that exhibits interesting ion pairing and solvation effects with the accompanying countercation. In most cases the center for such ion pairing is the single bridging carbonyl group, since the oxygen atoms of bridging carbonyl groups

---

* We are pleased to dedicate this manuscript to Prof. Erwin Weiss in recognition of his many important contributions to the field of organometallic chemistry.

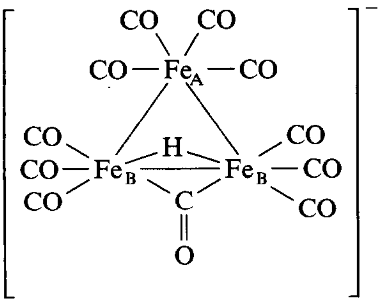

(I)

are more basic than those of terminal carbonyl groups [1]. Thus in the alkali metal salts $MHFe_3(CO)_{11}$ (M = Li, Na, K, Rb, Cs) spectroscopic studies [2], particularly shifts in infrared $\nu(CO)$ frequencies, indicate ion pairing of the alkali-metal cation with the bridging carbonyl oxygen of the $HFe_3(CO)_{11}^-$ anion. In addition, there is spectroscopic evidence [3] for ion pairing in the tertiary ammonium derivative $[Et_3NH][HFe_3(CO)_{11}]$ by hydrogen bonding from the N–H hydrogen of the Et_3NH^+ cation to the bridging CO oxygen of the $HFe_3(CO)_{11}^-$ anion.

The situation in the case of the secondary ammonium derivatives $[R_2NH_2]$-$[HFe_3(CO)_{11}]$ is more interesting since the $R_2NH_2^+$ cation has two potential hydrogens for hydrogen bonding but there is only one bridging carbonyl group in $HFe_3(CO)_{11}^-$ to act as a hydrogen bond acceptor. In the case of $[^iPr_2NH_2]$-$[HFe_3(CO)_{11}]$, prepared in aqueous solution [4], a structure determination by X-ray diffraction indicates that in the $^iPr_2NH_2^+$ cation one N–H group is hydrogen bonded to the bridging carbonyl group and the other N–H group is hydrogen bonded to a terminal carbonyl group. We have now isolated $[Cx_2NH_2]$-$[HFe_3(CO)_{11}] \cdot OEt_2$ (Cx = cyclohexyl) from the reaction of Cx_2NBBr_2 with $Na_2Fe_2(CO)_8$ in diethyl ether. Determination of the structure of $[Cx_2NH_2]$-$[HFe_3(CO)_{11}] \cdot OEt_2$ by X-ray diffraction indicates that in the $Cx_2NH_2^+$ cation, one N–H group is hydrogen bonded as usual to the bridging CO group of $HFe_3(CO)_{11}^-$ but the other N–H group is hydrogen-bonded to the diethyl ether thereby underscoring the weakness of hydrogen bonding to terminal CO groups as compared with bridging CO groups.

This paper reports the details of the structure determination of $[Cx_2NH_2]$-$[HFe_3(CO)_{11}] \cdot OEt_2$ by X-ray diffraction as well as a comparison of the Mössbauer effect spectrum of the $HFe_3(CO)_{11}^-$ anion with that of $Fe_3(CO)_{12}$.

Experimental section

The general experimental procedure is similar to that described in previous papers from this laboratory [5] except that infrared spectra were run on a Digilab FTS-60 Fourier transform infrared spectrometer.

Isolation of $[Cx_2NH_2][HFe_3(CO)_{11}] \cdot OEt_2$

The sample of $[Cx_2NH_2][HFe_3(CO)_{11}] \cdot OEt_2$ used in this work was isolated from an unsuccessful attempt to prepare dicyclohexylaminoboron iron carbonyl derivatives by the reaction of equimolar quantities of Cx_2NBBr_2 [6] (66 g, 190 mmol) and $Na_2Fe_2(CO)_8$ [7] (72 g, 190 mmol) in diethyl ether (600 ml) at −78°C. After warming to room temperature, the solvent was removed in vacuum. The hexane-insoluble residue was extracted with diethyl ether. Column chromatography using ether as an eluent gave 15.7 g (17% yield based on iron) of dark purple $[Cx_2NH_2][HFe_3(CO)_{11}] \cdot OEt_2$; carbon-13 NMR in $CDCl_3$: δ 221 and 210 from the carbonyl groups, δ 64.5, 29.5, and 23.8 from the cyclohexyl groups, and δ 54.3 and 14.2 from the diethyl ether. Anal. Found: C, 42.8; H, 4.9; N, 1.9. $C_{27}H_{35}Fe_3NO_{12}$ calc.: C, 44.2; H, 4.8; N, 1.9%.

The sample of $[Cx_2NH_2][HFe_3(CO)_{11}]$ used for the infrared spectroscopic studies was obtained from $[Cx_2NH_2]Cl$ and $KHFe_3(CO)_{11}$ in water similar to a published procedure [4].

Structure determination of $[Cx_2NH_2][HFe_3(CO)_{11}] \cdot OEt_2$ by X-ray diffraction

A crystal of $[Cx_2NH_2][HFe_3(CO)_{11}] \cdot OEt_2$ from diethyl ether was mounted on a Syntex P3 automated diffractometer. Unit cell dimensions (Table 1) were determined by least squares refinement of the best angular positions for fifteen independent reflections ($2\theta > 15°$) during normal alignment procedures using molybdenum radiation ($\lambda = 0.71069$ Å). Data (5979 independent points after removal of space group forbidden and redundant data) were collected at room temperature using a variable scan rate, a θ–2θ scan mode, and a scan width of 1.2° below K_{α_1} and 1.2° above K_{α_2} to a maximum 2θ value of 50°. Backgrounds were measured at each side of the scan for a combined time equal to the total scan time. The intensities of three standard reflections were remeasured after every 97 reflections. As the intensities of these reflections showed less than 5% variation, corrections for decomposition were deemed unnecessary. Data were corrected for Lorentz, polarization, and background effects. Observed reflections [3305 ($I > 3.0\sigma(I)$)] were used for solution of nonhydrogen positions of the structure by direct methods using

Table 1

Crystal data for $[Cx_2NH_2][HFe_3(CO)_{11}] \cdot O(C_2H_5)_2$

Formula	$Fe_3C_{27}H_{35}NO_{12}$
MW	733.1
a	17.449(5) Å
b	16.345(5) Å
c	13.466(4) Å
α	90.0°
β	118.45(2)°
γ	90.0°
V	3376.6(17) Å^3
$F(000)$	1512
μ(Mo-K_α)	13.26 cm^{-1}
λ(Mo-K_α)	0.71069 Å
D_{calc}	1.442 g cm^{-3}
Z	4
Space group	$P2_1/a$
Obs. refl.	3305
Octants meas.	$\pm h, k, l$
R/R_w	6.4/7.9%
G.O.F.	0.39

SHELX86 [8]. Refinements [9] of scale factor, positional, and isotropic thermal parameters for these atoms were carried out to convergence. The asymmetric unit consists of one HFe$_3$(CO)$_{11}^-$ ion which is hydrogen bonded to one hydrogen atom of a Cx$_2$NH$_2^+$ cation. The second hydrogen of Cx$_2$NH$_2^+$ is hydrogen bonded to the oxygen atom of an Et$_2$O molecule. The Et$_2$O molecule is disordered and shows two

Table 2

Non-hydrogen positional parameters for [Cx$_2$NH$_2$][HFe$_3$(CO)$_{11}$]·OEt$_2$

Atom	$x(\sigma(x))$	$y(\sigma(y))$	$z(\sigma(z))$
Fe1	−0.2883(1)	0.3204(1)	0.2495(1)
Fe2	−0.1226(1)	0.3467(1)	0.3298(1)
Fe3	−0.2015(1)	0.2386(1)	0.1613(1)
O11	−0.3472(5)	0.4100(5)	0.3869(8)
O12	−0.4203(5)	0.3899(6)	0.0339(7)
O13	−0.3874(5)	0.1720(4)	0.2315(7)
O14	−0.1743(4)	0.2440(4)	0.4649(5)
O21	−0.0624(6)	0.4665(6)	0.2160(7)
O22	−0.0469(5)	0.4325(5)	0.5435(6)
O23	0.0204(5)	0.2296(5)	0.4106(7)
O31	−0.3497(6)	0.1578(6)	−0.0245(8)
O32	−0.2369(6)	0.3887(6)	0.0262(7)
O33	−0.1671(6)	0.1027(4)	0.3239(8)
O34	−0.0545(6)	0.1937(7)	0.1269(9)
N1	−0.0976(4)	0.2380(4)	0.7035(6)
C1	0.8089(9)	0.6110(12)	0.4821(13)
C2	−0.3067(13)	0.1231(16)	0.6151(19)
C4	−0.2428(16)	0.1041(16)	0.7692(21)
C5	0.8145(13)	0.0928(11)	0.8809(13)
C11	−0.3250(6)	0.3755(6)	0.3337(9)
C12	−0.3650(7)	0.3637(7)	0.1168(10)
C13	−0.3492(6)	0.2294(6)	0.2363(8)
C14	−0.1890(5)	0.2836(5)	0.3812(8)
C21	−0.0885(7)	0.4201(7)	0.2544(9)
C22	−0.0774(6)	0.4015(6)	0.4564(8)
C23	−0.0375(6)	0.2754(7)	0.3764(9)
C31	−0.2915(8)	0.1886(8)	0.0496(12)
C32	−0.2216(7)	0.3331(8)	0.0835(9)
C33	−0.1810(7)	0.1564(7)	0.2633(9)
C34	−0.1116(8)	0.2115(9)	0.1401(11)
O38	−0.2517(17)	0.1604(17)	0.7013(31)
O39	−0.2251(16)	0.1419(17)	0.7106(28)
C111	−0.0162(6)	0.1867(6)	0.7441(9)
C112	−0.0431(7)	0.1026(7)	0.6939(11)
C113	0.0365(9)	0.0503(7)	0.7229(14)
C114	0.0956(9)	0.0893(9)	0.6833(14)
C115	0.1211(8)	0.1729(8)	0.7298(13)
C116	0.0430(7)	0.2259(6)	0.7057(10)
C121	−0.0876(6)	0.3216(5)	0.7569(7)
C122	−0.1685(6)	0.3704(6)	0.6851(8)
C123	−0.1593(7)	0.4551(7)	0.7373(11)
C124	−0.1409(8)	0.4530(7)	0.8567(11)
C125	−0.0627(8)	0.4007(7)	0.9252(10)
C126	−0.0720(7)	0.3154(6)	0.8760(8)

50% occupancy positions for the oxygen atom. Disorder of the carbon atoms attached to the oxygen is apparent. However, attempts to resolve this in terms of partial occupancy carbon positions were unsuccessful. The position of the hydrogen atom bridging Fe1 and Fe2 was apparent from a difference Fourier synthesis; however, this position was unstable to refinement. Hydrogen positions for dicyclohexyl and ammonium protons were calculated assuming idealized geometries and a C–H distance of 0.97 Å. Hydrogen atoms of the Et_2O moiety were ignored owing to the uncertainty of the carbon atom positions. Final cycles of least squares refinement allowed refinement of nonhydrogen positions with anisotropic thermal parameters. Parameters for hydrogen atoms were included with fixed isotropic thermal parameters. The function minimized, $\Sigma(|F_o| - |F_c|)^2$, led to a final agreement factor, $R = 6.4\%$ where $R = (\Sigma || F_o| - |F_c|| / \Sigma |F_o|) \times 100$. Scattering factors were taken from Cromer and Mann [10]. Anomalous dispersion corrections were introduced for Fe [11]. In the final stages of refinement a weight of $1/\sigma(F)^2$ was used: $R_w = 7.9\%$. Positional parameters and selected bond distances and angles are given in Tables 2 and 3, respectively. Tables of all bond distances and angles, anisotropic thermal parameters, and F_{obs} and F_{calc} are available from the authors upon request.

Mössbauer effect studies

The Mössbauer effect spectra were obtained on a constant-acceleration spectrometer which used a room temperature rhodium matrix cobalt-57 source and was calibrated at room temperature with α-iron foil. The Mössbauer effect absorbers were prepared by dispersing $[Cx_2NH_2][HFe_3(CO)_{11}] \cdot OEt_2$ uniformly in vaseline with a concentration of either 24 or 59 mg/cm^2 of sample. Different absorber concentrations were used in order to avoid saturation effects at 78 K and to produce a significant percent effect at 295 K. The spectra were fit by using standard computer least squares minimization techniques with two doublets whose components had equal linewidths. The components of the inner doublet had equal areas, but the components of the outer doublet had different areas.

Results and discussion

Structural studies

The sample of $[Cx_2NH_2][HFe_3(CO)_{11}] \cdot OEt_2$ was isolated inadvertently from an attempt to prepare dicyclohexylaminoboron iron carbonyl derivatives from the reaction of Cx_2NBBr_2 with $Na_2Fe_2(CO)_8$ in diethyl ether and identified by its structure determined by X-ray diffraction. This structure (Fig. 1) shows both the $Cx_2NH_2^+$ cation and the $HFe_3(CO)_{11}^-$ anion with the expected geometries. Of particular interest is the participation of the two hydrogen atoms of the $Cx_2NH_2^+$ cation in hydrogen bonding (Table 4). One of the hydrogen atoms H1 is hydrogen bonded to the oxygen atom of the single bridging CO group of $HFe_3(CO)_{11}^-$, namely O14, similar to a reported [4] hydrogen bond in $[^iPr_2NH_2][HFe_3(CO)_{11}]$. However, the other hydrogen atom H2 of the $Cx_2NH_2^+$ cation in $[Cx_2NH_2][HFe_3(CO)_{11}] \cdot OEt_2$ is hydrogen bonded to a diethyl ether oxygen (O38 or O39) whereas the other hydrogen atom of the $^iPr_2NH_2^+$ cation in $[^iPr_2NH_2][HFe_3(CO)_{11}]$ is hydrogen bonded to a terminal CO group [4]. This is in accord with the higher basicity of oxygen atoms of bridging CO groups relative to terminal CO groups [1]. Thus

Table 3

Selected bond distances (Å) and angles (°) for $[Cx_2NH_2][HFe_3(CO)_{11}]\cdot OEt_2$

Fe1-Fe2	2.594(2)	Fe3-Fe1-C11	168.3(3)
Fe2-Fe3	2.681(2)	Fe3-Fe1-C12	93.7(5)
Fe1-Fe3	2.684(3)	Fe3-Fe1-C13	88.6(4)
Fe1-C11	1.79(1)	C11-Fe1-C12	96.4(5)
Fe1-C12	1.79(1)	C11-Fe1-C13	96.2(5)
Fe1-C13	1.79(1)	C12-Fe1-C13	95.9(4)
Fe1-C14	1.892(7)	C14-Fe2-C21	164.0(4)
Fe2-C21	1.84(1)	C14-Fe2-C22	89.6(5)
Fe2-C22	1.75(1)	C14-Fe2-C23	93.9(5)
Fe2-C23	1.75(1)	C14-Fe2-Fe1	46.7(2)
Fe2-C14	1.910(1)	C14-Fe2-Fe3	78.2(3)
Fe3-C31	1.77(1)	Fe1-Fe2-C21	117.8(3)
Fe3-C32	1.80(1)	Fe1-Fe2-C22	112.8(4)
Fe3-C33	1.83(1)	Fe1-Fe2-C23	128.7(4)
Fe3-C34	1.78(2)	Fe1-Fe2-Fe3	61.16(6)
C11-O11	1.12(2)	Fe3-Fe2-C21	97.6(4)
C12-O12	1.16(1)	Fe3-Fe2-C22	167.2(4)
C13-O13	1.13(1)	Fe3-Fe2-C23	82.6(2)
C14-O14	1.22(1)	C21-Fe2-C22	95.2(5)
C21-O21	1.13(2)	C21-Fe2-C23	100.9(6)
C22-O22	1.15(1)	C22-Fe2-C23	94.6(4)
C23-O23	1.16(1)	Fe1-Fe3-C31	98.4(6)
C31-O31	1.15(1)	Fe1-Fe3-C32	80.6(5)
C32-O32	1.14(2)	Fe1-Fe3-C33	89.0(4)
C33-O33	1.14(1)	Fe1-Fe3-C34	157.1(4)
C34-O34	1.13(2)	Fe2-Fe3-C31	155.7(5)
O14 ··· H1	1.81	Fe2-Fe3-C32	78.8(3)
H2 ··· O38	2.07	Fe2-Fe3-C33	90.6(3)
H2 ··· O39	1.84	Fe2-Fe3-C34	99.4(4)
C1-C2	1.30(3)	C31-Fe3-C32	93.1(5)
C2-O38	1.26(4)	C31-Fe3-C33	94.3(5)
C2-O39	1.42(3)	C31-Fe3-C34	104.0(7)
C4-O38	1.25(4)	C32-Fe3-C33	168.0(6)
C4-O39	1.15(5)	C32-Fe3-C34	93.6(7)
C4-C5	1.36(3)	C33-Fe3-C34	93.8(6)
		Fe1-C11-O11	179.4(8)
Fe2-Fe1-Fe3	61.01(6)	Fe1-C12-O12	173.7(13)
Fe1-Fe2-Fe3	61.16(6)	Fe1-C13-O13	177.6(11)
Fe1-Fe3-Fe2	57.83(6)	Fe2-C21-O21	174.8(9)
Fe1-C14-Fe2	86.0(4)	Fe2-C22-O22	175.3(9)
Fe1-C14-O14	137.1(8)	Fe2-C23-O23	177.7(10)
Fe2-C14-O14	136.6(6)	Fe3-C31-O31	178.2(13)
C14-Fe1-C11	90.6(4)	Fe3-C32-O32	174.0(10)
C14-Fe1-C12	167.4(5)	Fe3-C33-O33	176.6(12)
C14-Fe1-C13	93.7(4)	Fe3-C34-O34	179.5(19)
C14-Fe1-Fe2	47.3(3)	C1-C2-O38	130 (3)
C14-Fe1-Fe3	78.4(4)	C1-C2-O39	118 (2)
Fe2-Fe1-C11	108.5(3)	C2-O38-C4	95 (2)
Fe2-Fe1-C12	120.3(4)	C2-O39-C4	91 (2)
Fe2-Fe1-C13	132.1(3)	O38-C4-C5	132 (2)
Fe2-Fe1-Fe3	61.01(6)	C39-C4-C5	122 (3)

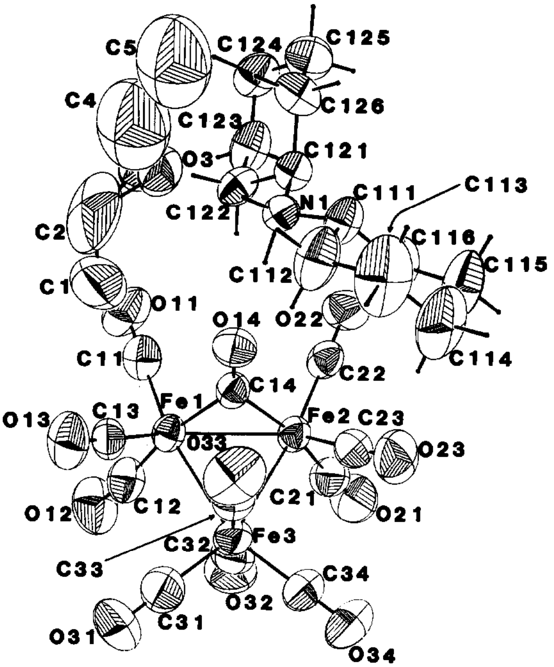

Fig. 1. ORTEP diagram of $[Cx_2NH_2][HFe_3(CO)_{11}] \cdot OEt_2$.

crystallization of a $[R_2NH_2][HFe_3(CO)_{11}]$ salt from diethyl ether can lead to rupture of a hydrogen bond to a terminal CO oxygen with formation of a hydrogen bond to the ether oxygen but does not affect the stronger hydrogen bond to the bridging CO oxygen. Table 4 also shows that the key features of the geometry of the $HFe_3(CO)_{11}^-$ anion are relatively insensitive to its hydrogen bonding to the counter cation.

The infrared ν(CO) frequency of the bridging CO group in $HFe_3(CO)_{11}^-$ salts has been used to indicate the participation of its oxygen atom in hydrogen bonding [4]. Thus bridging ν(CO) frequencies of 1740, 1650, and 1550 cm^{-1} have been taken as indications of the formation of zero, one, and two hydrogen bonds, respectively, between the bridging CO and the countercations. In $CHCl_3$ the bridging ν(CO) frequency of $[Cx_2NH_2][HFe_3(CO)_{11}]$ appears at 1654 cm^{-1} indicative of a single hydrogen bond to the bridging CO group as was found for the previously studied [4] $[R_2NH_2][HFe_3(CO)_{11}]$ derivatives (R = Et, ^{i}Pr). In the weakly basic Et_2O a complex pattern of bridging ν(CO) frequencies of 1779m, 1750w, 1684w, and 1655m cm^{-1} is observed for $[Cx_2NH_2][HFe_3(CO)_{11}]$ suggesting that Et_2O can partially displace hydrogen bonds to the bridging CO group. In the much more strongly basic tetrahydrofuran bridging ν(CO) frequencies of $[Cx_2NH_2][HFe_3(CO)_{11}]$ appear only at 1780w and 1748m cm^{-1} suggesting that tetrahydrofuran has completely displaced the hydrogen bonds to the bridging CO group in accord with reported [4] observations on $[R_2NH_2][HFe_3(CO)_{11}]$ (R = Et, ^{n}Bu, ^{i}Pr). The structure of $[Cx_2NH_2][HFe_3(CO)_{11}] \cdot OEt_2$ determined by X-ray diffraction indicates coexistence of hydrogen bonds to the bridging CO group and the ether oxygen suggesting similar stabilities of hydrogen bonds of both of these types. This is in accord with the

Table 4

Anion geometry and hydrogen bonding in different salts of $HFe_3(CO)_{11}^-$

Salt	Reference	X-ray R Factor	Anion geometry (Å or °)				Hydrogen bonding		
			Fe_A-Fe_A	Fe_A-Fe_B	C–O bridging	Fe–C–Fe	bridging N–H ··· CO	Other	Type
$[Ph_3PNPPh_3][HFe_3(CO)_{11}]$	[a]	0.053	2.572(2)	2.699(2)	1.202(13)	83.5(4)	none possible		
$[^iPr_2NH_2][HFe_3(CO)_{11}]$	[b]	0.076	2.579(2)	2.704(3) 2.709(3)	1.211(12)	84.6(4)	1.932	2.177	terminal CO
$[Cx_2NH_2][HFe_3(CO)_{11}]\cdot OEt_2$	this work	0.064	2.594(2)	2.681(2) 2.684(3)	1.22(1)	86.0(4)	1.81	1.84 2.07	Et_2O

[a] E. Iiskola, T.A. Pakkanen, T.T. Pakkanen and T. Vanäläinen, Acta Chim. Scand., A37 (1983) 125. [b] C.K. Chen, C.H. Cheng and T.H. Hseu, Organometallics, 6 (1987) 868.

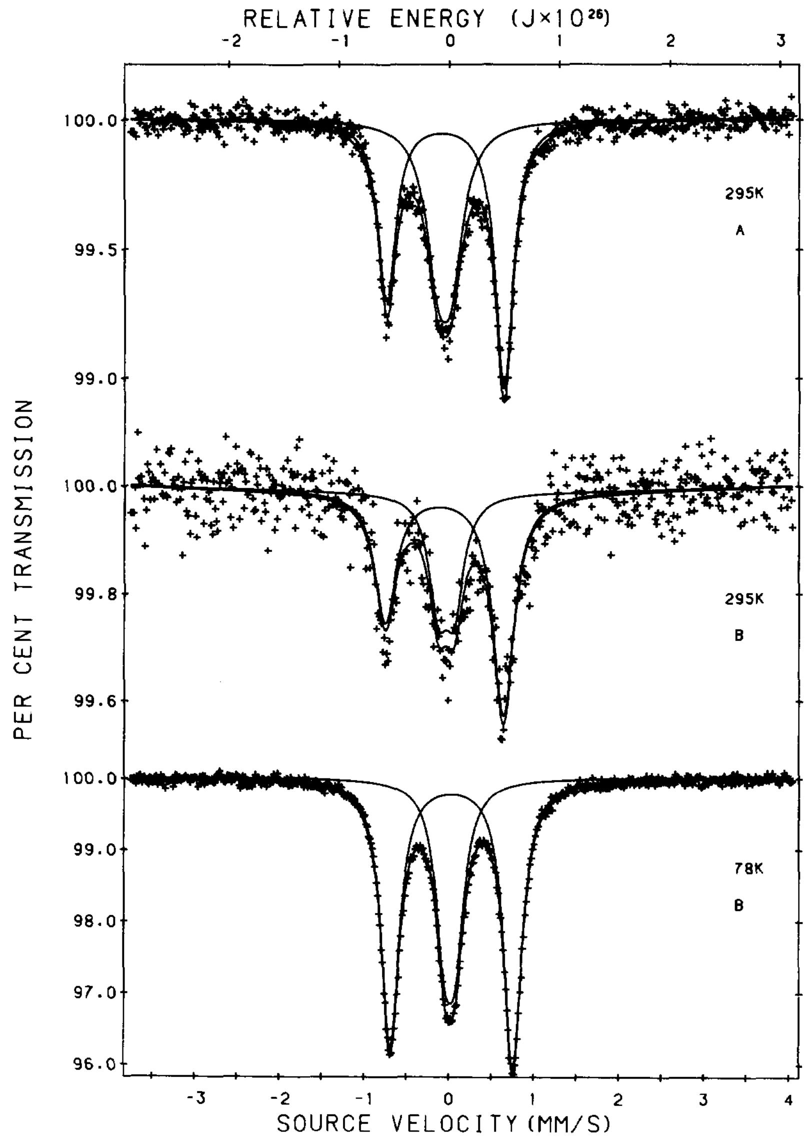

Fig. 2. Mössbauer spectra of $[Cx_2NH_2][HFe_3(CO)_{11}]\cdot OEt_2$ obtained at 295 and 78 K. The absorber thickness was 59 mg/cm^2 for the spectrum labeled A and 24 mg/cm^2 for the spectra labelled B.

infrared spectroscopic observation of both hydrogen bonded and non-hydrogen bonded bridging CO groups in diethyl ether solutions of $[Cx_2NH_2][HFe_3(CO)_{11}]$ mentioned above.

Mössbauer effect studies

The Mössbauer spectra of $[Cx_2NH_2][HFe_3(CO)_{11}]$ are shown in Fig. 2 and the resulting hyperfine parameters are given in Table 5. The parameters are similar to those obtained for $[Et_4N][HFe_3(CO)_{11}]$ and $Na[HFe_3(CO)_{11}]$, and the small differences, particularly in ΔE_Q, may result from different interactions with the differing cations [12–14].

The doublet with a small splitting and small area is assigned to Fe3 in the crystallographic structure shown in Fig. 1 corresponding to Fe_A in structure I. The doublet with the larger quadrupole splitting and the larger area is assigned to the two chemically equivalent but crystallographically distinct Fe1 and Fe2 sites. These assignments are consistent with those given in earlier work [12–15].

As is indicated in Table 5 there are both similarities and differences in the Mössbauer spectral hyperfine parameters for the $HFe_3(CO)_{11}^-$ anion and $Fe_3(CO)_{12}$. Because the magnitude of $\Delta E_{Q,A}$ increases with increasing temperature, it seems quite likely that the quadrupole interaction is negative in the $HFe_3(CO)_{11}^-$ anion as is the case in $Fe_3(CO)_{12}$. The quadrupole interaction at the two bridged sites, $\Delta E_{Q,B}$, is substantially larger in the $HFe_3(CO)_{11}^-$ anion than in $Fe_3(CO)_{12}$, indicating that the presence of the bridging hydrogen reduces the symmetry at this site. Upon formal reduction from $Fe_3(CO)_{12}$ to $HFe_3(CO)_{11}^-$ the isomer shift at each iron site in $HFe_3(CO)_{11}^-$ becomes more negative, corresponding to a higher *s*-electron density at the iron-57 nucleus, as would be expected by the replacement of a bridging carbonyl group with a bridging hydrogen. The influence of the hydrogen on reducing the isomer shift is largest for the bridged Fe1 and Fe2 sites in $HFe_3(CO)_{11}^-$, but the reduction is not insignificant even at the Fe3 site.

At 78 K the relative areas of the two spectral components in $HFe_3(CO)_{11}^-$ are 66% to 34%, which is very close to the expected 2:1 ratio. As the temperature is increased, the area of the bridged iron sites, Fe1 and Fe2, decreases relative to that of the unique iron site, Fe3. A similar change was observed [12] in $Fe_3(CO)_{12}$ and was attributed to a different temperature dependence of the recoil-free *f*-factor for the two sites. An analysis of the temperature dependence of both the isomer shift and the spectral absorption area [16,17] gives values for the effective absorber mass, M_{eff}, the Mössbauer lattice temperature, θ_M, and an estimate of the room temperature recoil-free *f*-factors. The results presented in Table 5 yield M_{eff} values of 113 and 124 g/mol, θ_M values of 58 and 66 K, and *f*-factors of 2.4×10^{-3} and 1.3×10^{-2} for the bridged iron sites and for the unique iron site in $HFe_3(CO)_{11}^-$, respectively. When the *f*-factors are very small it is most likely that their temperature dependences can be quite different [15]. Indeed, the Fe1 and Fe2 sites have a very small *f*-factor which may also be associated with the nature of Fe–H–Fe bridge bonding and the difficulty in locating the hydrogen in the X-ray structure. The rather small *f*-factors are also consistent with the rather large thermal mean-square displacements observed in the X-ray structure. The other lattice parameters are quite typical for this type of very flexible organorion cluster [15,17–19].

One of the most striking features of the Mössbauer spectrum of $HFe_3(CO)_{11}^-$ is the asymmetry in the area of the two components of the quadrupole doublet resulting from the bridged Fe1 and Fe2 sites, an asymmetry which decreases upon cooling. This asymmetry has been observed earlier in $Fe_3(CO)_{12}$ and is attributed to a Goldanski–Karyagin effect resulting from an anisotropy in the recoil-free *f*-factors [15,20]. This anisotropy is clearly observed in the thermal mean-square displacement factors reported for $Fe_3(CO)_{12}$ [15,21]. It seems that a similar anisotropy in the recoil-free *f*-factors must be present in $HFe_3(CO)_{11}^-$. The thermal factors yield mean-square displacements U_{11}, U_{22}, and U_{33} of 0.027, 0.051, and 0.093 Å^2 for Fe1; 0.026, 0.052, and 0.097 Å^2 for Fe2; and 0.029, 0.061, and 0.146 Å^2 for Fe3. This

Table 5

Mössbauer effect spectral parameters

Compound	T (K)	δ_A [a] (mm/s)	$\Delta E_{Q,A}$ (mm/s)	Γ_A (mm/s)	Area %	δ_B [a] (mm/s)	$\Delta E_{Q,B}$ (mm/s)	Γ_B (mm/s)	A_1/A_4	Area (%)	A_A/A_B	Abs. Area [b] (%E) (mm/s)	Reference
$[Cx_2NH_2][HFe_3(CO)_{11}]$	295	−0.054	−0.16	0.32	42	−0.041	1.38	0.25	0.67	58	1.38	0.46	this work
	78	0.019	−0.13	0.26	34	0.039	1.44	0.26	0.90	66	1.94	4.60	this work
$[Et_4N][HFe_3(CO)_{11}]$	80	0.01	0.16	0.30	–	0.03	1.41	0.28	–	–	–	–	13,14
$Na[HFe_3(CO)_{11}]$	298	−0.08	0	–	–	−0.10	1.32	–	–	–	–	–	12
$Fe_3(CO)_{12}$	295	−0.012	−0.197	0.31	46	0.022	0.944	0.26	0.78	54	1.16	–	15
	78	0.078	−0.079	0.34	39	0.133	1.116	0.27	0.96	61	1.59	–	15

[a] Relative to room-temperature natural α-iron foil. [b] Obtained from the 24 mg/cm^2 absorber spectrum.

anisotropy is somewhat larger than that found in $Fe_3(CO)_{12}$ and clearly accounts for the observed area asymmetry in the outer lines of the spectra shown in Fig. 2. As was pointed out earlier [15,20] compounds with very small recoil-free fractions, as is the case here, are most likely to show tha Goldanski–Karyagin asymmetry. Because the quadrupole interaction for the Fe3 site is so small, it is not possible to observe any asymmetry for the site.

Acknowledgment

The authors would like to thank Drs. F. Grandjean and A. Hautot for their help during the course of the Mössbauer studies. We are indebted to Prof. James de Haseth and his coworkers at the University of Georgia for assistance with the infrared spectra. We also acknowledge partial financial support of the work at the University of Georgia by the Air Force Office of Scientific Research (Grant AFOSR-84-0050) and of the University of Missouri-Rolla by the donors of the Petroleum Research Fund, administered by the American Chemical Society as well as a cooperative scientific research grant 86/685 from NATO.

References

1 C.P. Horwitz and D.F. Shriver, Adv. Organomet. Chem., 23 (1984) 219.
2 C.K. Chen and C.H. Cheng, Inorg. Chem., 22 (1983) 3378.
3 C.D. Pribula and T.L. Brown, J. Organomet. Chem., 71 (1974) 415.
4 C.K. Chen, C.H. Cheng and T.H. Hseu, Organometallics, 6 (1987) 868.
5 R.B. King, F.-J. Wu and E.M. Holt, J. Am. Chem. Soc., 109 (1987) 7764.
6 V.I. Spitsyn, I.D. Kolli, T.G. Sevast'yanova and E.A. Balabonova, Izv. Akad. Nauk. SSSR, Ser. Khim., (1974) 2626; Bull. Acad. Sci. USSR., Chem. Ser., (1974) 2535.
7 H. Strong, P.J. Krusic and J. San Filippo Jr., Inorg. Syn., 24 (1986) 157.
8 G. Sheldrick, SHELX86: Program of Crystal Structure Determination, University of Göttingen, Germany, 1986.
9 J.M. Stewart (Ed.), The XRAY System – Version of 1980, Technical Report TR446 of the Computer Center, University of Maryland, College Park, Maryland.
10 D.T. Cromer and I.B. Mann, Acta Crystallogr., A24 (1968) 321.
11 J. Ibers and W.C. Hamilton, International Tables for X-Ray Crystallography, Kynoch Press, Birmingham, 1984, Vol. IV.
12 N.E. Erickson and A.W. Fairhall, Inorg. Chem., 4 (1965) 1320.
13 K. Farmer, M. Kilner, R. Greatrex and N.N. Greenwood, J. Chem. Soc. A, (1969) 2339.
14 R. Greatrex and N.N. Greenwood, Discuss. Faraday Soc., 47 (1969) 126.
15 F. Grandjean, G.J. Long, C.G. Benson and U. Russo, Inorg. Chem., 27 (1988) 1524.
16 D.R. Wilson and R.H. Herber, J. Am. Chem. Soc., 106 (1954) 1646.
17 R.H. Herber, in R.H. Herber (Ed.), Chemical Mössbauer Spectroscopy, Plenum, New York, 1984, pp. 199–216.
18 H. Dorn, B.E. Hanson and E. Motell, Inorg. Chem. Acta, 54 (1981) L71.
19 B.E. Hanson, E.C. Lisic, J.T. Petty and G.A. Iannaconne, Inorg. Chem., 25 (1986) 4062.
20 F. Grandjean, G.J. Long, C.G. Benson and U. Russo, Hyperfine Interact., 40 (1988) 299.
21 F.A. Cotton and J.M. Troup, J. Am. Chem. Soc., 96 (1974) 4155.